Journal of Hazardous Materials 170 (2009) 27–34

Contents lists available at ScienceDirect

Journal of Hazardous Materials

journal homepage: www.elsevier.com/locate/jhazmat

Adsorption of dyes on Sahara desert sand

Canan Varlikli[a,*], Vlasoula Bekiari[b], Mahmut Kus[c], Numan Boduroglu[a], Ilker Oner[a], Panagiotis Lianos[d], Gerasimos Lyberatos[e], Siddik Icli[a]

[a] Ege University, Solar Energy Institute, Izmir, Turkey
[b] Technological Education Institute of Messolonghi, Department of Aquaculture and Fisheries, 30200 Messolonghi, Greece
[c] Selcuk University, Department of Chemical Engineering, Konya, Turkey
[d] University of Patras, Engineering Science Department, 26500 Patras, Greece
[e] Chemical Engineering Department, University of Patras, 26500 Patras, Greece

ARTICLE INFO

Article history:
Received 8 October 2008
Received in revised form 17 April 2009
Accepted 3 May 2009
Available online 15 May 2009

Keywords:
Sahara desert sand
Adsorption
Dyes
Water treatment

ABSTRACT

Sahara desert sand (SaDeS) was employed as a mineral sorbent for retaining organic dyes from aqueous solutions. Natural sand has demonstrated a strong affinity for organic dyes but significantly lost its adsorption capacity when it was washed with water. Therefore, characterization of both natural and water washed sand was performed by XRD, BET, SEM and FTIR techniques. It was found that water-soluble kyanite, which is detected in natural sand, is the dominant factor affecting adsorbance of cationic dyes. The sand adsorbs over 75% of cationic dyes but less than 21% for anionic ones. Among the dyes studied, Methylene Blue (MB) demonstrated the strongest affinity for Sahara desert sand (Q_e = 11.98 mg/g, for initial dye solution concentration 3.5×10^{-5} mol/L). The effects of initial dye concentration, the amount of the adsorbent, the temperature and the pH of the solution on adsorption capacity were tested by using Methylene Blue as model dye. Pseudo-first-order, pseudo-second-order and intraparticle diffusion models were applied. It was concluded that adsorption of Methylene Blue on Sahara desert sand followed pseudo-second order kinetics. Gibbs free energy, enthalpy change and entropy change were calculated and found −6411 J/mol, −30360 J/mol and −76.58 J/mol K, respectively. These values indicate that the adsorption is an exothermic process and has a spontaneous nature at low temperatures.

© 2009 Elsevier B.V. All rights reserved.

1. Introduction

Industrial processes, such as dyeing of textile fibers and printing, use synthetic organic dyes that often cause environmental pollution. Removing these dyes from industrial wastes is essential from many points of view. In recent years, Sahara desert sand (SaDeS) has become the subject of investigations related with its influence on the lower atmosphere and its effects on oceanographic equilibrium. Many of these studies have reported that SaDeS has the capacity of adsorbing and carrying volatile organics [1–5]. Although this fact is known, there are not many studies in the literature treating adsorption itself, while there are no studies focusing on removal of industrial wastes by the use of SaDeS [6]. In view of the limited supply of water in countries of northern Africa, where SaDeS is abundant, use of this natural material for cleaning waste waters may be of great value.

In the recent years several works have appeared in the scientific literature reporting adsorption of several dyes, most notably among them, Methylene Blue (MB), by both natural and synthetic sorbents [7–17]. The adsorption of MB has become an index of adsorption performance for adsorbents, because of its low cost and availability in abundance [11,12]. In the present work, the adsorption capacity of SaDeS on some anionic (Acid Orange-7, Congo Red, Eriochrome Black T and Rose Bengal) and cationic (Janus Green, Rhodamine 6G, Toluidine Blue and MB) dyes was studied and by using MB as a model dye, the effect of adsorbent amount, initial dye concentration, temperature and pH on its adsorption capacity were determined.

2. Experimental

2.1. Materials

All chemicals were purchased from Aldrich and Merck and were used as received. Water was purified by using a Millipore installation. The chemical structures of the dyes used in this work are shown in Fig. 1. SaDeS was collected in Tozeur, Tunisia. After collection, stones and other heavy particles were removed from the sample, then crunched, ground and sieved through a 230 mesh sieve.

* Corresponding author. Tel.: +90 232 3884000/1244; fax: +90 232 3886027.
E-mail address: canan.varlikli@ege.edu.tr (C. Varlikli).

0304-3894/$ – see front matter © 2009 Elsevier B.V. All rights reserved.
doi:10.1016/j.jhazmat.2009.05.030

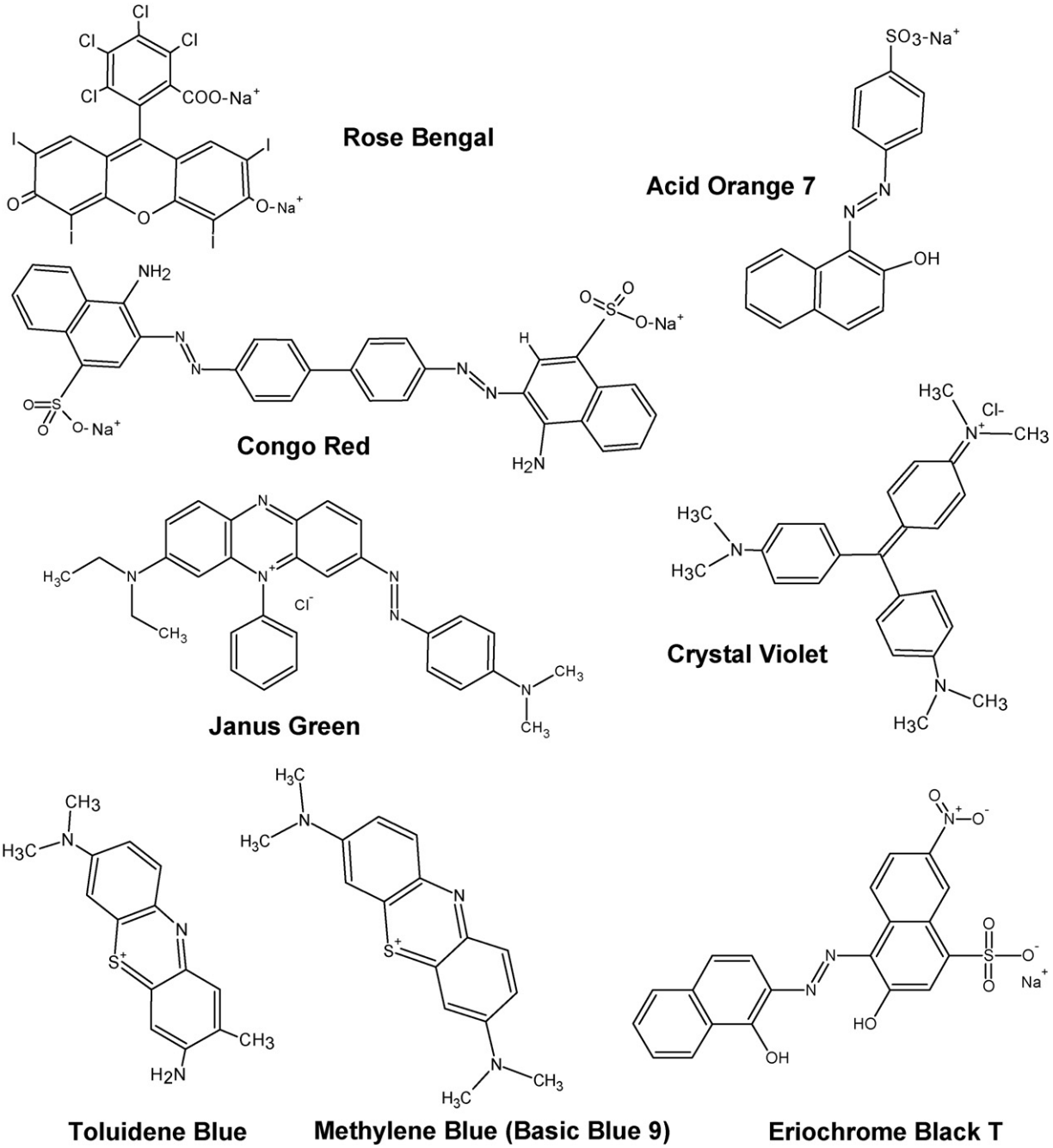

Fig. 1. Chemical structures of the dyes studied in this work.

2.2. Instruments

UV–vis absorption measurements were recorded by using an Analytic Jena S 600 UV spectrophotometer. X-ray diffraction (XRD) spectra were obtained with a Phillips X'pert Pro spectrometer (CuK radiation $\lambda = 1.56^{\circ}$). SEM images were registered by using a Phillips XL-30S FEG microscope. FTIR measurements were made with a PerkinElmer Spectrum BX-FTIR spectrophotometer. Specific surface area was measured with a Quantachrome Autosorb automated nitrogen adsorption system.

2.3. Characterization of SaDeS

The N_2 surface area of SaDeS was found to be $15\,m^2/g$. For this study we considered natural, water washed (250 mg SaDeS in 100 ml of distilled water, stirred for 2 h and filtered, 10 times), calcinated (450 °C, 4 h in oven) and UV treated ($1000\,W/m^2$ Xe lamb, 12 h) SaDeS. Among them, by using the same adsorbent amount, dye concentration and initial volume of solution, natural SaDeS gave the maximum adsorption capacity. In the case of MB, comparing with natural SaDeS, we obtained a decrease in adsorption capacity of 63%, 30% and 46% in water washed, UV and heat treated sand, respectively. Apparently, natural SaDeS contains some water-soluble and UV and heat degradable active components, that increase its adsorption capacity. At this point of the study, taking the significant decrease in adsorption capacity into account, we tried to identify the structural changes that SaDeS goes through following water treatment. As can be seen in Fig. 2, natural SaDeS reveals an ordered, needle-like structure, which vanished after the dust was washed.

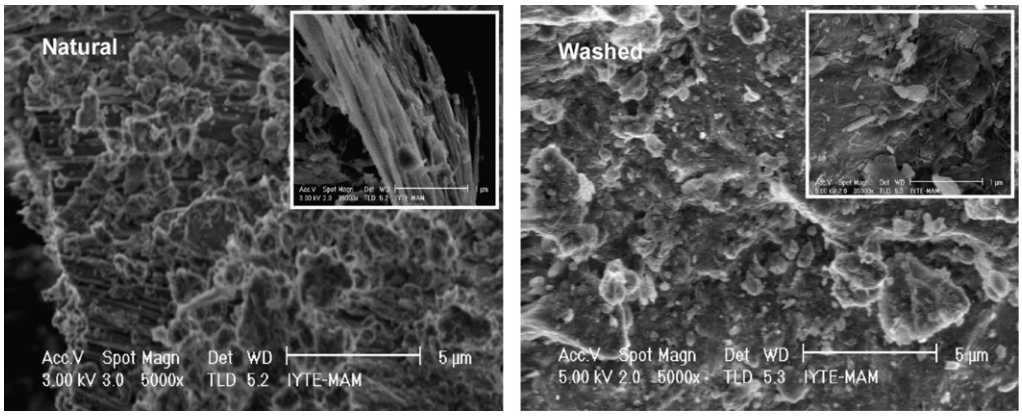

Fig. 2. SEM images of natural and washed SaDeS.

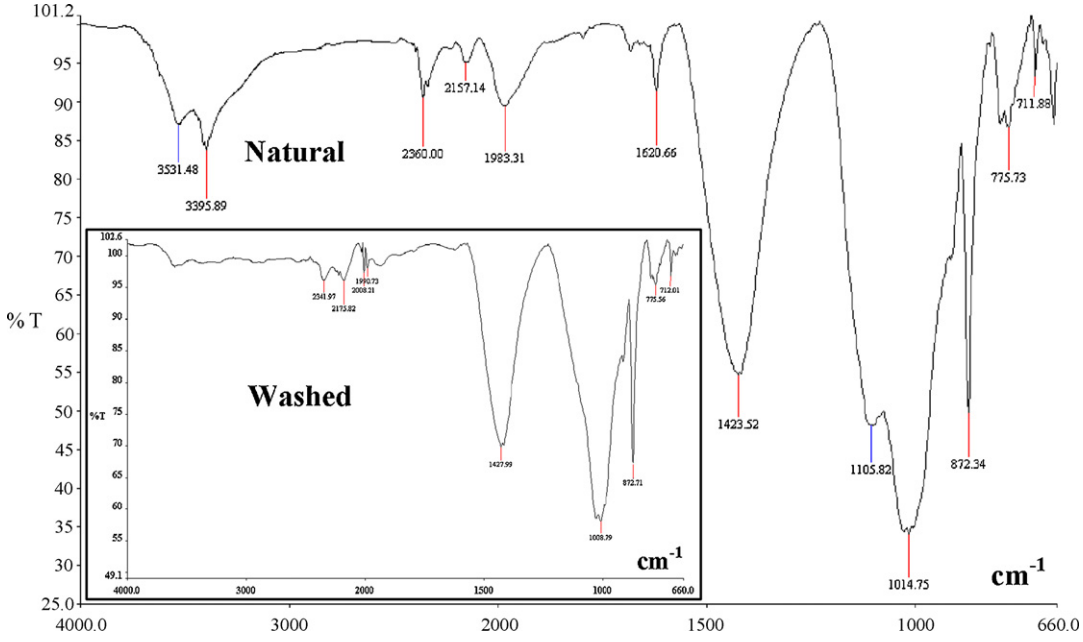

Fig. 3. FTIR spectra of natural and washed SaDeS.

In order to explain these data, it was necessary to carry out a characterization of both natural and washed SaDeS. FTIR and XRD analyses of natural and washed SaDeS are shown in Figs. 3 and 4, respectively. The information provided by these spectra is summarized in Table 1. The basic components present in natural SaDeS are calcite, SiS_2, quartz, sjoegrenite and kyanite. After washing, calcite and quartz were still there, while SiS_2, kyanite (Al_2SiO_5) and sjoegrenite $\{[Mg_6Fe_2(OH)_{16}CO_3(H_2O)_{4.5}]_{0.25}\}$ were no longer detected. In addition, an increase of the quantity of SiO_2 was detected. Increase of SiO_2 is probably due to the production of silica by the following reaction: $SiS_2 + 2H_2O \rightarrow SiO_2 + 2H_2S$ [18]. It is interesting at this point to note the data of Fig. 5. Fig. 5 shows that when SaDeS was submerged in water, the pH value of the supernatant increased. This was expected since Sahara dust is known to increase the pH of rain drops [1]. However, at relatively high SaDeS concentrations the maximum pH value of the supernatant water was lower. It is then highly probable, that the formation of SiO_2 and H_2S is responsible for this pH differentiation.

Table 1
Data obtained by analysis of SaDeS by XRD and FTIR.

Component	Natural		Washed	
	XRD[a]	FTIR	XRD	FTIR
Calcite	+	1420–1430 cm^{-1} CO_3	+	1420–1430 cm^{-1} CO_3
Silicon sulfide	+	1105 cm^{-1} Si–S stretching	–	1010 cm^{-1} Si–O dominant silica peak
Quartz [25]	+	775–795 cm^{-1} doublet	+	775–795 cm^{-1} doublet
Sjoegrenite[b] [26]	+	3530 and 1620 cm^{-1} O–H stretching of MgOH and FeOH	–	Disappeared
Kyanite [27]	+	3385–3410 cm^{-1} triplet	–	Disappeared

[a] Presence of the components is determined by using Philips X'pert Pro spectrometers library.
[b] One may think that the peaks attributed to sjoegrenite are due to hygroscopic water. If that was the case, those bands should have been seen in washed SaDeS sample as the two samples were dried in the same conditions.

Table 2
Parameters for the effect of initial dye concentration and temperature for MB.

Initial dye concentration C_0, mol/L (mg/L)	Temperature (°C)	Q_e (experimental; mg/g)	Pseudo-first-order model			Pseudo-second-order model				Intra particle diffusion		
			Q_e (calculated; mg/g)	r^2	k (min^{-1})	Q_e (calculated; mg/g)	r^2	k (g/mg min)	h (mg/g min)	k_i (mg/g $min^{1/2}$)	r^2	c
3.5×10^{-5} (13.08)	RT	11.98	3.74	0.9054	0.076	12.16	0.9999	0.061	9.02	4.115	0.9733	1.021
3.0×10^{-5} (11.21)	RT	10.21	2.86	0.9311	0.107	10.39	0.9998	0.098	10.58	3.713	0.9893	0.643
2.5×10^{-5} (9.35)	RT	8.26	2.39	0.832	0.087	8.38	0.9999	0.121	8.49	3.109	0.9462	0.847
2.0×10^{-5} (7.48)	RT	6.35	1.91	0.7855	0.196	6.41	0.9992	0.245	10.06	2.9814	0.9685	0.006
1.5×10^{-5} (5.61)	RT	3.89	1.14	0.7963	0.510	3.85	1.0	2.26	33.52	1.892	0.9183	0.949
3.5×10^{-5} (13.08)	30	11.80	5.12	0.8995	0.1308	12.16	0.9999	0.061	9.02	3.791	0.9544	1.5221
	40	11.46	8.58	0.9511	0.2042	12.03	0.9962	0.057	8.25	1.376	0.9147	6.032
	50	11.52	3.47	0.8859	0.1151	11.79	0.9999	0.0815	11.32	3.963	0.9606	1.361
	60	11.67	2.77	0.8058	0.1149	11.81	0.9998	0.1277	17.81	3.820	0.887	2.747

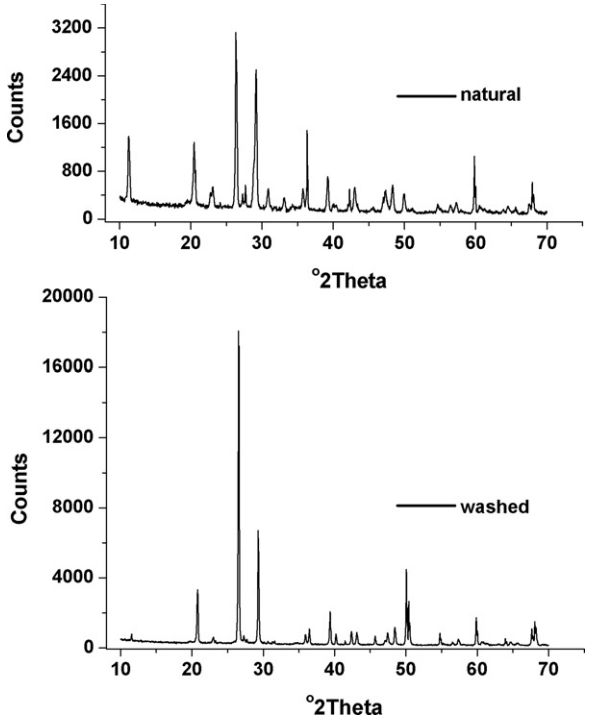

Fig. 4. XRD spectra of natural and washed SaDeS.

It has been observed that SaDeS quantities over 15 mg/25 ml water do not cause a significant change in pH of the suspension. Therefore, in the adsorption studies of the dyes, the solution volume and the natural SaDeS amount were fixed to 25 ml and 20 mg, respectively. The pH of 25 ml water containing 20 mg of SaDeS, measured by the use of WTW pH/Cond 340i, is 8.24.

2.4. Models for adsorption, kinetic and thermodynamic studies

The amount of dye adsorbed (Q_e) at equilibrium was calculated by using the equation [19–21]:

$$Q_e = \frac{(C_0 - C_e)V}{m} \quad (1)$$

where, C_0 is the initial dye concentration (in mg/L), V is the volume of the solution (in L) and m is the mass of the adsorbent (in g). Adsorption data were fitted to a Langmuir isotherm which has been used for many adsorption processes of monolayer adsorption

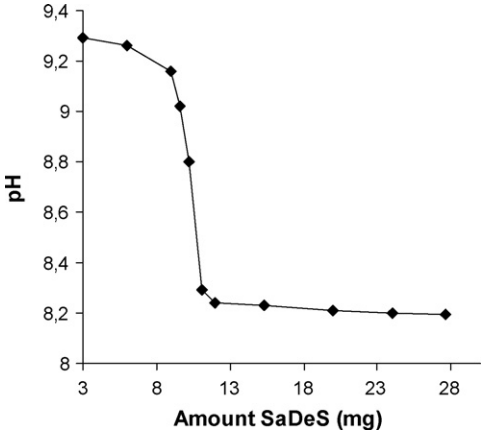

Fig. 5. Variation of pH of 25 ml water containing SaDeS as a function of SaDeS quantity.

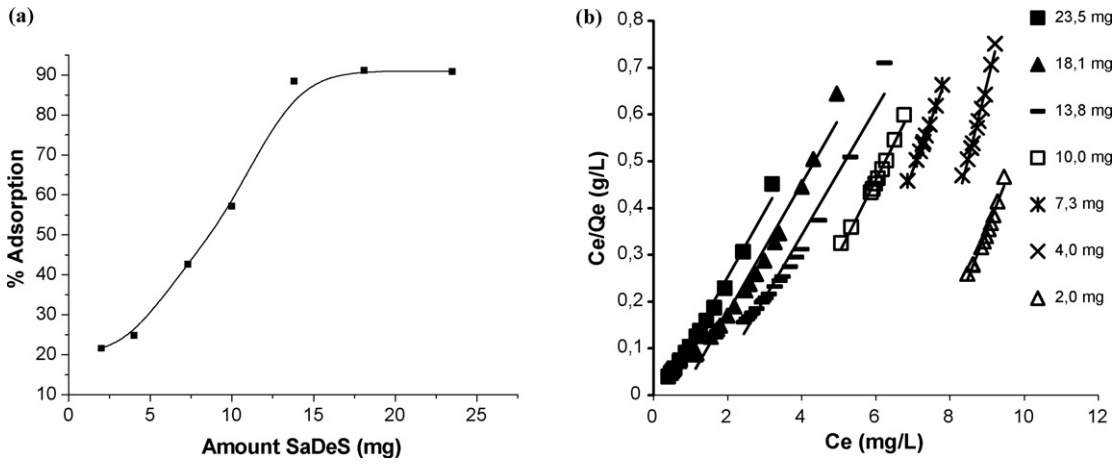

Fig. 6. (a) Variation of percentage adsorption values of MB on SaDeS (b) analysis of Langmuir isotherm – variation of the ratio C_e/Q_e versus C_e ([MB] = 3×10^{-5} M; contact time = 50 min; room temperature).

[10,22]:

$$\frac{C_e}{Q_e} = \left(\frac{1}{Q_m K_L}\right) + \left(\frac{C_e}{Q_m}\right) \quad (2)$$

where Q_m is the monolayer capacity. By plotting C_e/Q_e versus C_e the Langmuir constant (K_L) was obtained.

Pseudo-first-order and pseudo-second-order models have been widely used in understanding the dye kinetics [13–16]. These models were tested for the adsorption of MB on SaDeS and the best model was selected depending on the linear regression correlation coefficient, r^2, values.

Pseudo-first-order model has been described by Lagergren [23]:

$$\log(Q_e - Q_t) = \frac{\log\ Q_e - kt}{2.303} \quad (3)$$

where Q_t is the amount of dye adsorbed at a time (mg dye/g SaDeS) and k is the equilibrium rate constant (min^{-1}). The application of this kinetic model gave r^2 value of 0.9311.

Pseudo-second-order model was also applied using the equation below (Ho's pseudo-second-order model) [24]:

$$\frac{t}{Q_t} = \frac{1}{kQ_e^2} + \frac{t}{Q_e} \quad (4)$$

where k is the rate constant of second-order adsorption (g/mg min) and kQ_e^2 is the initial adsorption rate constant (h). The application of the pseudo-second-order model gave r^2 values of 0.999.

For calculating the rate constant of intraparticle diffusion the equation:

$$Q_t = k_i t^{1/2} + c \quad (5)$$

was used, where k_i is the intraparticle diffusion rate constant (mg/g $min^{1/2}$). This constant was calculated from the slope of the straight-line portions of the plots, Q_t versus $t^{1/2}$. The intercept of this plot, c, is proportional to the extent of boundary layer thickness [16]. The obtained values are presented in Table 2 at different initial dye concentrations and temperatures.

Thermodynamic properties, such as the Gibbs free energy change (ΔG°, J/mol), enthalpy change (ΔH°, J/mol) and entropy change (ΔS°, J/mol K) were obtained from the experiments carried out at different temperatures and by the use of following equations [10,22]:

$$\Delta G^\circ = -RT \ln\ K_L \quad (6)$$

$$\ln K_L = -\frac{\Delta G^\circ}{RT} = \left(\frac{\Delta S^\circ}{R}\right) - \left(\frac{\Delta H^\circ}{RT}\right) \quad (7)$$

Table 3
Adsorption percentages of the dyes by SaDeS (λ, wavelength of maximum light absorption by the aqueous solution of the dye).

Dye (cationic)	λ (nm)	Ads (%)	Dye (Anionic)	λ (nm)	Ads (%)
Methylene Blue	665	91	Congo Red	490	21
Toluidine Blue	630	84	Eriochrome Black T	620	20
Janus Green	664	84	Rose Bengal	525	≅1
Rhodamine 6G	533	76	Acid Orange-7	483	≅1

A plot of $\ln K_L$ versus $1/T$ should be a straight-line with a slope of $-(\Delta H^\circ/R)$ and an intercept of $(\Delta S^\circ/R)$. R is the universal gas constant (8.3145 J/mol K).

3. Results and discussion

3.1. Adsorption, kinetic and thermodynamic studies

Concentration of the dyes was arranged in order to have absorption values of 0.7–0.8. Although the time period applied is 50 min, it is observed that the maximum change in absorption percentage occurs within the first 10 min. The maximum adsorption percentages and wavelength of maximum light absorbance of the dyes are given in Table 3. It is observed that SaDeS is a strong adsorbent for cationic dyes. Anionic dyes are weakly adsorbed while some of them are not adsorbed at all. Table 4 shows the adsorption capacity of MB dye in other systems for comparison. In the literature, it is known that kyanite is capable of adsorbing positively charged material by electrostatic attraction [28]. Therefore it is assumed that kyanite is the major factor affecting the adsorbent properties of SaDeS and the significant decrease in adsorption capacity of the sand following water treatment is attributed to the kyanite loss.

Since maximum percentage of adsorption was obtained for MB (Table 3.) and since MB has been used as a model compound in many other reports [7–17], we have chosen this dye for further studies of

Table 4
Adsorption capacity of MB dye in various systems.

Sorbent	Ads (%)	Q_e (mg/g)	Reference
Fly ash	58	40 for C_0 = 65 mg/L	[7b]
Guava (*Psidium guajava*) leaf powder	96	295 for C_0 = 300 mg/L	[10]
Sand	92	–	[12]
Wheat cells	95	76 for C_0 = 100 mg/L	[13]
Peat	90	90 for C_0 = 200 mg/L	[17]

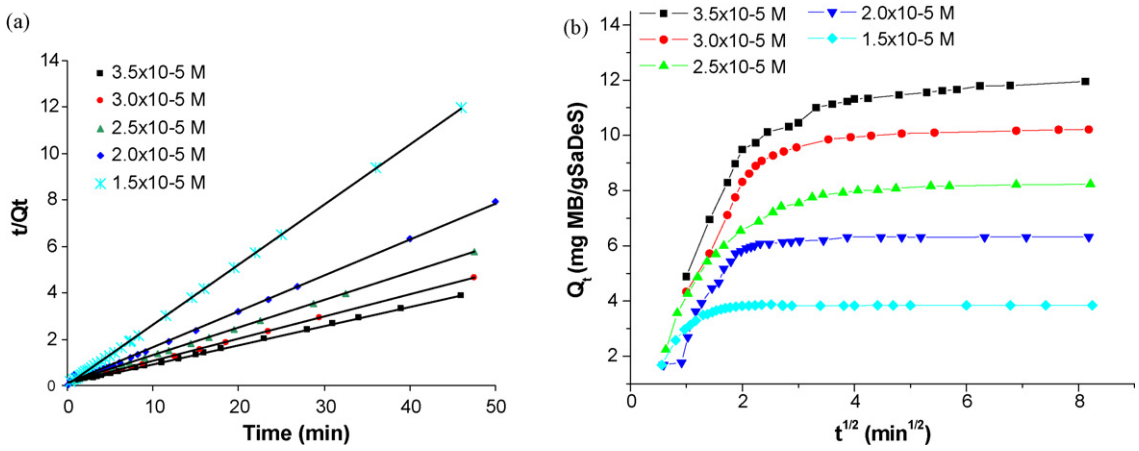

Fig. 7. (a) Ho's second-order model application for MB adsorption on SaDeS and (b) intraparticle diffusion plot for the removal of MB from aqueous solution.

adsorption mechanisms on SaDeS by examining the influence of different experimental parameters.

3.1.1. Effect of adsorbent amount

Adsorbent amount is an important parameter in the determination of adsorption capacity. The effect of the adsorbent amount is investigated by addition of various amounts of SaDeS in 25 ml 3.5×10^{-5} M MB aqueous solution, at room temperature and at constant time interval (50 min). It is observed that the percentage of adsorption increases approximately until 20 mg of SaDeS and a 10-fold increase in the adsorbent amount results in a 4-fold increase in the adsorption percentage (Fig. 6a) and a 4-fold decrease in the amount of dye adsorbed per unit mass of the adsorbent. This observation is attributed in literature to the fact that adsorption sites remain unsaturated [13].

When the adsorption data obtained by the use of various quantities of SaDeS in a 3.5×10^{-5} M MB solution, are fitted to the Langmuir equation (Eq. (2)), the best fit is observed for SaDeS quantities of higher than 18.1 mg/25 ml water (Fig. 6b). This finding supports our choice of 20 mg SaDeS per 25 ml of dye solution for further investigations.

3.1.2. Effect of concentration

The adsorption capacity of SaDeS for MB was studied for five different initial dye concentrations as shown in Table 2. The results indicated that the adsorption capacity increases with increasing the initial dye concentration. When the dye concentration increased from 1.5×10^{-5} M to 3.5×10^{-5} M at room temperature (*RT*), the amount of adsorbed dye increased from 3.89 mg/g to 11.98 mg/g, respectively (Table 2). For an initial dye concentration 1.5×10^{-4} M, the loading capacity of the adsorbent increased to 41.5 mg/g.

At this point of our study we applied the pseudo-first-order and the pseudo-second-order models for the five different initial dye concentrations and the results are presented in Table 2. Both models basically include all steps of adsorption such as external film diffusion, adsorption and internal particle diffusion [9,11]. As we can see, the correlation coefficients obtained for the pseudo-first-order model were between 0.7855 and 0.9311, while for the pseudo-second order model were almost equal to unity. When the initial dye concentration changed from 3.5×10^{-5} M to 1.5×10^{-5} M, the initial adsorption rate, h, increased from 9.02 to 33.52 whereas the rate constant, k, also increased from 0.061 to 2.26. In addition to the r^2 values, the amount of adsorbed dye at equilibrium, Q_e, calculated from pseudo-second-order model, is more comparable with the experimental data, with only a minor deviation being apparent. Fig. 7a shows the linearized plot of the pseudo-second-order model, indicating the pseudo-second-order nature of the adsorption. The obtained plot with the use of Eq. (4) is given in Fig. 7b. In this plot, the initial linear portion is attributed to bulk diffusion, and the second to intraparticle/pore diffusion [10]. Although the r^2 values of intraparticle diffusion are also above 0.9, and the k_i values are increasing with the increasing initial dye concentration, the intercept values obtained are not proportional to the initial dye concentration. It is known in literature that intraparticle diffusion model is better fitted to denser solids like activated clay and/or chitosan flakes and small molecules obey the pseudo-second-order

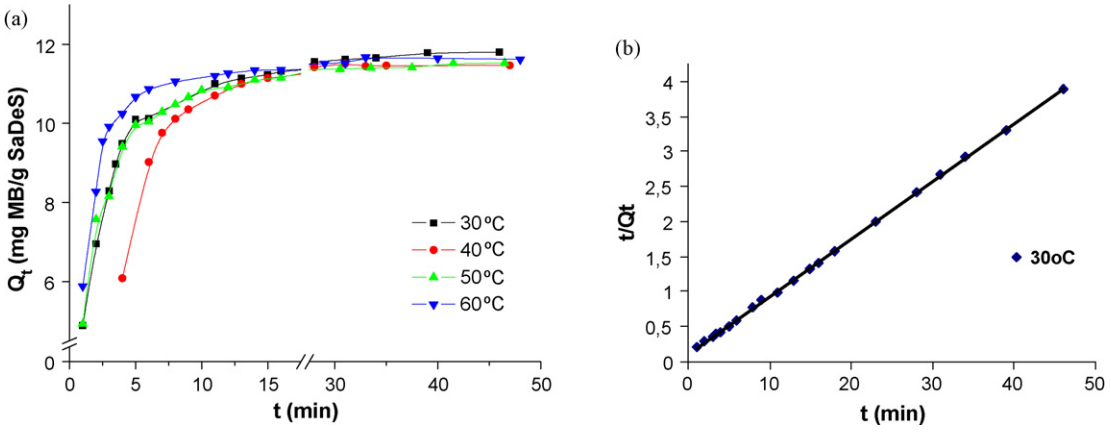

Fig. 8. (a) The variation of the amount of dye adsorbed with adsorption time at different temperatures and (b) application of Ho's second-order model for MB adsorption on SaDeS at 30 °C.

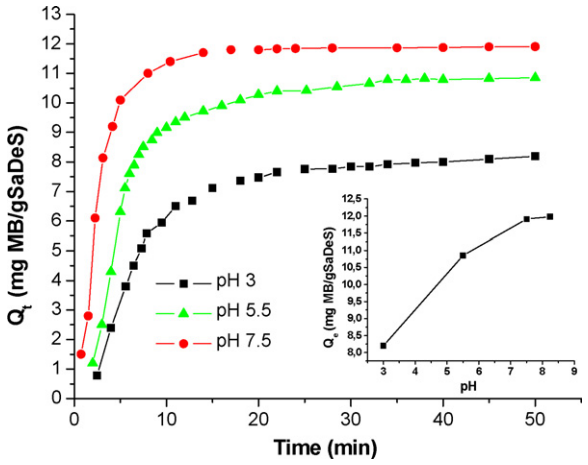

Fig. 9. The effect of initial suspension pH on the adsorption of 3×10^{-5} M MB onto SaDeS (inset; experimental Q_e values versus pH. Q_e value at pH 8.24 is abstracted from Fig. 7b and Table 1).

model [10,11]. Our results also show that, being a small molecule, MB adsorbs on SaDeS following pseudo-second-order kinetics.

3.1.3. Effect of temperature

Temperature is an important factor affecting the adsorption rate and dye uptake. The temperature effect on the adsorption of MB onto SaDeS is studied by the use of 3.5×10^{-5} M MB at 30 °C, 40 °C, 50 °C and 60 °C. The increase in temperature leads to slight changes in Q_e values (Fig. 8). The Q_e value decreases from 11.80 mg/g to 11.46 mg/g when the temperature is raised from 30 °C to 40 °C, suggesting an exothermic adsorption (Table 2). However, when the temperature is increased from 40 °C to 60 °C, the Q_e value increases from 11.46 mg/g to 11.67 mg/g, suggesting an endothermic adsorption (Table 2). For the pseudo-second-order model, the rate constant, k, and initial adsorption rate, h, increase significantly with increasing temperature from 30 °C to 60 °C. The k value changes from 0.061 to 0.1277, while the h value changes from 9.02 to 17.81. No matter whether the adsorption is endothermic or exothermic, an increase in the rate constant is always expected with the increase in temperature. Therefore, equilibrium dye uptake values have to be considered to actually determine whether the adsorption is exothermic or endothermic. However, the uptake amount of MB on SaDeS does not give a clear dependence on temperature. This situation is attributed to several reasons in the literature such as the ionization state of various surface groups of adsorbents with a change in temperature [29] (Fig. 9).

3.1.4. Effect of pH

The hydrogen ion concentration of the suspension affects the degree of ionization of the dye and the surface properties of the adsorbents [22]. Therefore it is one of the important factors that affect the adsorption capacity of the sorbent. The effect of initial suspension pH on the adsorption of 3.5×10^{-5} M MB onto SaDeS is investigated at the pHs of 3, 5.5 and 7.5 (Fig. 10). The pH was adjusted using 0.1 M HCl and 0.1 M NaOH solutions. It is observed that at low pHs, the rate of the adsorption and the total amount of adsorbed dye decrease, as the negative charge on SaDeS tends to saturate by protons. This finding is in good agreement with many other reports published on MB adsorption [30].

3.1.5. Thermodynamic parameters

Thermodynamic parameters of ΔH°, ΔS° and ΔG° are calculated from the corresponding plots of Eqs. (6) and (7). The plot (Fig. 10) has r^2 value of 0.9666. The obtained values are given in Table 5. The negative values of ΔS°, ΔH° and ΔG° suggest that the overall

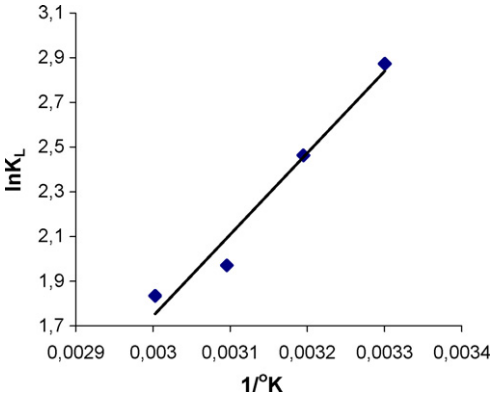

Fig. 10. The plot obtained from Eq. (7) to calculate thermodynamic parameters (ΔH°, ΔS° and ΔG°).

Table 5
Thermodynamic parameters for the adsorption of MB on SaDeS.

T (K)	ΔG° (J/mol)	ΔH° (J/mol)	ΔS° (J/mol K)
303	−7236		
313	−6411	−30,360	−76.58
323	−5294		
333	−5080		

adsorption of MB onto SaDeS has a decreased randomness at the solid/solution interface, and is an exothermic spontaneous process at low temperatures [31].

4. Conclusions

Natural SaDeS contains active components that can strongly adsorb positively charged organic material from an aqueous solution. For the present SaDeS, which was collected in Tozeur, Tunisia, the active component was related with kyanite, a negatively charged mineral that imparts electrostatic attraction towards cationic material. Washed SaDeS loses its active component while its original microstructure is lost. More than 90% of MB may be removed from a 3.5×10^{-5} M 25 ml solution with the use of 20 mg of adsorbent. The adsorption is found to be pseudo-second-order. The present study indicates that natural SaDeS is a good candidate as a low cost adsorbent to be used for the removal of dyes from water.

Acknowledgements

We are thankful to Prof. Dr. Cemal Saydam for kindly providing the SaDeS and Prof. Dr. Serdar Ozcelik for the SEM images. Financial aid from the GR-TR Bilateral R&T Cooperation program is graciously acknowledged.

References

[1] A.S. Goudie, N.J. Middleton, Saharan dust storms: nature and consequences, Earth-Sci. Rev. 56 (2001) 179–204.
[2] Y. Erel, U. Dayan, R. Rabi, Y. Rudich, M. Stein, Trans boundary transport of pollutants by atmospheric mineral dust, Environ. Sci. Technol. 40 (2006) 2996–3005.
[3] (a) M. Kocak, N. Mihalopoulos, N. Kubilay, Chemical composition of the fine and coarse fraction of aerosols in the northeastern Mediterranean, J. Atmos. Environ. 41 (2007) 7351–7368;
(b) A.C. Saydam, I. Polar, The impact of Saharan dust on the occurrence of algae blooms, Ecol. Environ. 36 (1999) (ISBN: 1-85312-742-6).
[4] C.R. Usher, A.E. Michel, V.H. Grassian, Reactions on mineral dust, Chem. Rev. 103 (2003) 4883–4939.
[5] G. Pan, M.D. Krom, B. Herut, Adsorption–desorption of phosphate on airborne dust and riverborne particulates in east Mediterranean seawater, Environ. Sci. Technol. 36 (2002) 3519–3524.

[6] A. Zertal, M. Jacquet, B. Lavédrine, T. Sehili, Photodegradation of chlorinated pesticides dispersed on sand, Chemosphere 58 (2005) 1431–1437.
[7] (a) B.K. Singh, N.S. Rawat, Comparative sorption equilibrium studies of toxic phenols on fly ash and impregnated fly ash, J. Chem. Technol. Biotechnol. 61 (1994) 307–317;
(b) K. Rastogi, J.N. Sahu, B.C. Meikap, M.N. Biswas, Removal of methylene blue from wastewater using fly ash as an adsorbent by hydrocyclone, J. Hazard. Mater. 158 (2008) 531–540.
[8] W.-T. Tsai, H.-C. Hsu, T.-Y. Su, K.-Y. Lin, C.-M. Lin, Removal of basic dye (methylene blue) from wastewaters utilizing beer brewery waste, J. Hazard. Mater. 154 (2008) 73–78.
[9] A.Z. Aroguz, J. Gulen, R.H. Evers, Adsorption of methylene blue from aqueous solution on pyrolyzed petrified sediment, Bioresour. Technol. 99 (2008) 1503–1508.
[10] V. Ponnusami, S. Vikram, S.N. Srivastava, Guava (*Psidium guajava*) leaf powder: novel adsorbent for removal of methylene blue from aqueous solutions, J. Hazard. Mater. 152 (2008) 276–286.
[11] M.-Y. Chang, R.-S. Juang, Adsorption of tannic acid, humic acid, and dyes from water using the composite of chitosan and activated clay, J. Colloid Interface Sci. 278 (2004) 18–25.
[12] S.B. Bukallah, M.A. Rauf, S.S. AlAli, Removal of Methylene Blue from aqueous solution by adsorption on sand, Dyes Pigments 74 (2007) 85–87.
[13] Y. Bulut, H. Aydın, A kinetics and thermodynamics study of methylene blue adsorption on wheat shells, Desalination 194 (2006) 259–267.
[14] A. Gürses, Ç. Doğar, M. Yalçın, M. Açıkyıldız, R. Bayrak, S. Karaca, The adsorption kinetics of the cationic dye, methylene blue, onto clay, J. Hazard. Mater. B131 (2006) 217–228.
[15] N. Kannan, M.M. Sundaram, Kinetics and mechanism of removal of methylene blue by adsorption on various carbons—a comparative study, Dyes Pigments 51 (2001) 25–40.
[16] M. Dogan, M. Alkan, Adsorption kinetics of methyl violet onto perlite, Chemosphere 50 (2003) 517–528.
[17] A.N. Fernandes, C.A.P. Almeida, C.T.B. Menezes, N.A. Debacher, M.M.D. Sierra, Removal of methylene blue in aqueous solution by peat, J. Hazard. Mater. 144 (2007) 412–419.
[18] I. Tomaszkiewicz, G.A. Hope, P.A.G. O'Hare, A fluorine bomb calorimetric determination of the standard molar enthalpy of formation of silicon disulfide SiS_2(cr) at the temperature 298.15 K. Enthalpies of dissociation of Si–S bonds, J. Chem. Thermodyn. 29 (1997) 1031–1045.
[19] A. Sayari, S. Hamoudi, Y. Yang, Applications of pore-expanded mesoporous silica. 1. Removal of Heavy metal cations and organic pollutants from wastewater, Chem. Mater. 17 (2005) 212–216.
[20] S. Duran, D. Solpan, O. Guven, Synthesis and characterization of acrylamide-acrylic acid hydrogels and adsorption of some textile dyes, Nucl. Instrum. Methods Phys. Res. B 151 (1999) 196–199.
[21] V. Bekiari, P. Lianos, Ureasil gels as a highly efficient adsorbent for water purification, Chem. Mater. 18 (2006) 4142–4146.
[22] M.J. Iqbal, M.N. Ashiq, Adsorption of dyes from aqueous solutions on activated charcoal, J. Hazard. Mater. 139 (2007) 57–66.
[23] S. Lagergren, Zur theorie der sogenannten adsorption gelöster stoffe Kungliga Svenska Vetenskapsakademiens, Handlingar 24 (1898) 1–39.
[24] Y.S. Ho, G. McKay, Sorption of dye from aqueous solution by peat, Chem. Eng. J. 70 (1998) 115–124.
[25] A. Adamczyk, M. Handke, W. Mozgawa, FTIR studies of $BPO_4{\cdot}2SiO_2$, $BPO_4{\cdot}SiO_2$ and $2BPO_4{\cdot}SiO_2$ joints in amorphous and crystalline forms, J. Mol. Struct. 511–512 (1999) 141–144.
[26] R.L. Frost, S. Bahfenne, J. Graham, Infrared and infrared emission spectroscopic study of selected magnesium carbonate minerals containing ferric iron-Implications for the geosequestration of greenhouse gases, Spectrochim. Acta Part A: J. Mol. Biol. Spectrosc. 71 (2008) 1610–1616.
[27] A. Wieczorek, E. Libowitzky, A model fort he OH detect incorporation in kyanite based on polarised IR spectroscopic investigations, Schweizerische Mineralogishe und Petrographische Mitteilungen 84 (2004) 333–343.
[28] M. Ajmal, R.A.K. Rao, R. Ahmad, J. Ahmad, L.A.K. Rao, Removal and recovery of heavy metals from electroplating wastewater by using Kyanite as an adsorbent, J. Hazard. Mater. B87 (2001) 127–137.
[29] M.I. El-Khaiary, Kinetics and mechanism of adsorption of methylene blue from aqueous solution by nitric-acid treated water-hyacinth, J. Hazard. Mater. 147 (2007) 28–36.
[30] C.-Huang Weng, Y.-Fong Pan, Adsorption of a cationic dye (methylene blue) onto spent activated clay, J. Hazard. Mater. 144 (2007) 355–362.
[31] M. Zhaoa, Z. Tang, P. Liu, Removal of methylene blue from aqueous solution with silica nano-sheets derived from vermiculite, J. Hazard. Mater. 158 (2008) 43–51.